Journal of Hydrology, 135 (1992) 73–86
Elsevier Science Publishers B.V., Amsterdam

mhp 144

[3]

Determining soil hydrologic properties from rain simulator or double ring infiltrometer experiments: a comparison

J. Touma and J. Albergel

Centre ORSTOM de Dakar B.P. 1386, Dakar, Senegal

(Received 1 June 1991; accepted 25 October 1991)

ABSTRACT

Touma, J. and Albergel, J., 1992. Determining soil hydrologic properties from rain simulator or double ring infiltrometer experiments: a comparison. J. Hydrol., 135: 73–86.

Two infiltration experiments were conducted on two plots of 1 m^2, each equipped with a neutron meter access tube and tensiometers. One infiltration was performed with a constant head of water maintained at the soil surface, the other using a rain simulator. The order of experiments was reversed on the two plots, i.e. on the first plot, simulated rain preceeded infiltration under constant head, while on the second plot, ponded infiltration was performed prior to the simulated rain. For each plot, the water pressure and hydraulic conductivity relationships versus water content were determined from both experiments for the various horizons of the soil profile. It is shown that the range of data obtained from the double ring infiltrometer is much wider than that corresponding to the rain simulator. This is due probably to surface sealing during the latter experiment. Application of the Van Genuchten model (1980) to predict the hydraulic conductivity from the water retention curve shows good agreement for some horizons but is not satisfactory for others. It is concluded that when the soil surface is subject to crusting, the double ring infiltrometer is more suitable than the rain simulator for the determination of soil hydrologic properties.

INTRODUCTION

Ring infiltrometers are commonly used for in situ determination of soil hydraulic properties (i.e. the water content–pressure head relationship, or water retention curve $h(\theta)$, and the relation between water content and hydraulic conductivity, $K(\theta)$), measurement of infiltration capacity (Ahuja et al., 1976; Chong et al., 1981; Youngs, 1986) and determination of spatial variability of soil properties (Vieira et al., 1981; Vauclin et al., 1983). On the other hand, rain simulators are widely used to study soil erosion (Bryan and De Ploey, 1983; Miller, 1987; Remley and Bradford, 1989), soil crusting

Correspondence to: J. Touma, Centre ORSTOM de Dakar, B.P. 1386, Dakar, Senegal.

0022-1694/92/$05.00

(Agassi et al., 1981; Sharma et al., 1981; Levy et al., 1986), as well as infiltration and runoff (Swartzendruber and Hillel, 1975; Agassi et al., 1982; Bridge and Ross, 1985; Bach et al., 1986), but rarely to determine soil hydraulic properties in situ. To the authors' knowledge, the only attempt to do this was that of Jeppson et al. (1975). Even in that case, only the water retention curve was measured directly while the $K(\theta)$ relationship was obtained merely by matching field data with a numerical model. Similarly, very few studies exist concerning the comparison of field infiltration capacity obtained from both types of experiments (Julander and Jackson, 1983; Ben-Hur et al., 1987). The purpose of this study is to compare results derived from the two experiments. The site is located in the Sine Saloum valley (Senegal). The soil is sandy in the upper 50 cm: about 6% fine particles (< 0.02 mm). The percentage of fine particles increases to 30% at 100 cm depth.

MATERIALS AND METHODS

The rain simulator

This device is described in detail by Casenave (1982) and Bernard (1987). A nozzle, hanging 4 m above the soil surface, oscillates at a constant angular velocity and is supplied at a constant rate with water. The jet of droplets produced by the nozzle is a pyramid, the base of which at the soil surface is $(1.5 \times 0.25)\,m^2$. The size distribution and kinetic energies of the droplets compare closely with those of natural rain (Asseline and Valentin, 1978). The intensity of the simulated rain can be adjusted between 20 and 180 mm h^{-1} by changing the angle of oscillation of the nozzle. The irrigated surface varies between $(4.5 \times 1.5)\,m^2$ and $(1.5 \times 1.5)\,m^2$, according to the intensity of the simulated rain.

Rain intensity and cumulative runoff measurements are performed on a $1\,m^2$ plot delimited by a square metallic frame driven 10 cm deep in the soil. The centre of the frame and the nozzle lie on the same verticle. In addition, two of the frame's sides are parallel to the axis of oscillation of the nozzle, which in turn is in the direction of the maximum topographic slope. The downhill side of the frame is provided with 20 holes regularly spaced, each 1 cm diameter. They collect runoff in a furrow protected from the simulated rain by a cap and lead it into a reservoir 1 m away from the plot. The reservoir is $0.1\,m^2$ section and is equipped with a water level recorder.

Cumulative runoff, and thus cumulative infiltration, are measured with a nominal precision of 0.1 mm. The oscillation and water supply of the nozzle as well as the water level recorder are activated simultaneously. Simulated rain

can be applied either at constant intensity or according to a storm pattern. In the latter case, intensity varies instantaneously in a stepwise manner. Up to ten different intensities may be programmed prior to the experiment.

The double-ring infiltrometer

The metallic frame of the rain simulator forms the 'inner ring' after obstruction of the runoff collection holes. The 'outer ring' is formed by an earth dyke 10 cm high surrounding the frame. A plastic sheet placed vertically in the centre of the dyke ensures that it is impervious. The size of this outer ring is approximately the same as that irrigated by the rain simulator at the highest intensity; $(1.5 \times 2.0)\,m^2$. Each plot is equipped with an access tube for a neutron probe in its centre. Ten tensiometers are placed vertically at 10, 20, 30, 40, 60, 80, 100, 120, 140 and 160 cm depth. The distance between each tensiometer and the access tube is not less than 25 cm in order not to affect the sphere of influence of the neturon meter. Neutron measurements are made from 10 to 180 cm depth with a step of 10 cm; the neutron probe has been calibrated previously with a special calibration curve for the 10 cm depth.

The experiments

On the first plot, a series of three simulated rains 12 h apart, followed by 50 days of redistribution, preceded the ponded infiltration experiment. The first two rains correspond to a constant intensity ($60\,mm\,h^{-1}$), the third one reproduced the typical storm pattern of the region with a 10 year return period. The order of experiments was reversed on the second plot, i.e. ponded infiltration followed by 50 days of redistribution preceded the simulated rain experiments performed according to the same scheme. Redistribution was allowed to perform under the 'internal drainage' conditions, i.e. with the soil surface covered by a plastic sheet to prevent surface evaporation (Hillel et al., 1972), for the first 10 days and under 'natural conditions', i.e. with surface evaporation allowed by removal of the sheet, (Arya et al., 1975; Vachaud et al., 1978) thereafter. Infiltration under ponded conditions was initiated by manual ponding to 4 cm depth and maintained by subsequent manual topping up when the ponding depth at the soil surface dropped to 3.5 cm. On each plot, the cumulative infiltration during the series of simulated rains was practically the same as that observed under ponded conditions, i.e. 16 cm for the first plot and 18 cm for the second. Neutron measurements were not possible during infiltration under simulated rain, neither were they performed during ponded infiltration. Thus all results presented in this paper were obtained during redistribution.

RESULTS AND DISCUSSION

For the two plots, the results obtained from both experiments compare closely, therefore only those corresponding to the second plot will be detailed below.

The water retention relation

This relationship is obtained by relating the water content $\theta(t, z_0)$ and pressure head $h(t, z_0)$ measurements made at the same time at the same depth z_0. Note that this assumes vertical flow conditions, which is realistic in view of the size of the plot and the location of the access tube as well as of the tensiometers (Touma, 1984).

Figure 1(a) shows values obtained from the rain simulation experiment (denoted SR) and Fig. 1(b) those inferred from the ponded infiltration experiment (PI). These results allow four horizons to be distinguished in the profile: 10 (asterisks), 20–40 (open symbols), 60 (plusses) and $\geqslant 80$ cm (solid symbols). Figures 2(a)–2(d), show for each of the four horizons respectively, the $h(\theta)$ points obtained from both experiments. Obviously, taking the experimental errors into account, no distinction can be made between points obtained from SR or those determined from PI. However, the range of variation of the measured variables especially in the upper horizons, depends on the water supply mode at the soil surface. For $z = 10$ cm, while the maximum value of water content recorded during SR does not exceed 0.23, it is greater than 0.28 during PI. Clearly, under simulated rain the soil upper horizons were not saturated, even though runoff was observed. Most probably, this is due to surface sealing which occurs frequently with this type of experiment (Hardy et al., 1983).

To examine the influence of the limited range of measured data during SR at $z = 10$ cm, an analytical expression of the form proposed by Van Genuchten (1980)

$$\theta = (\theta_s - \theta_r)/(1 + (ah)^b)^c + \theta_r \qquad (1)$$

with $c = 1 - 1/b$ was fitted on the observed data. Note that this equation is a generalization of the one proposed originally (with $c = 1$) by Gardner (1958). In this relation θ_s and θ_r are the saturation and the so-called residual water contents, a and b are constants. Although θ_r may be measured experimentally, it is determined here by curve fitting as well as a and b (Van Genuchten, 1980). Fitting was carried out using the Marquardt technique (1963), without linearizing eqn. (1). Even though θ_s was not measured in either experiment, manual extrapolation of available PI data allows the estimation

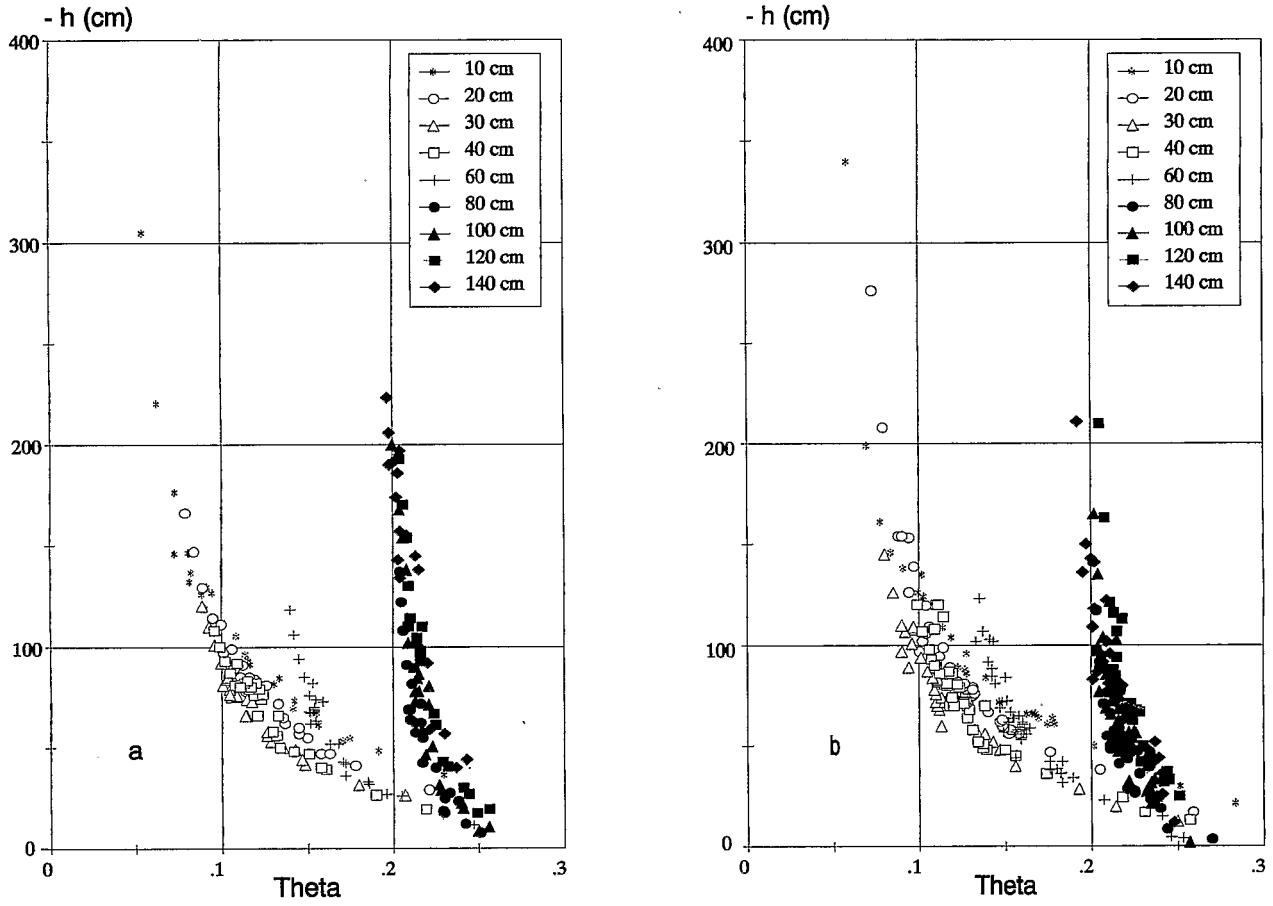

Fig. 1. $h(\theta)$ for the various depths obtained from the simulated rain (a) and the ponded infiltration (b) experiments.

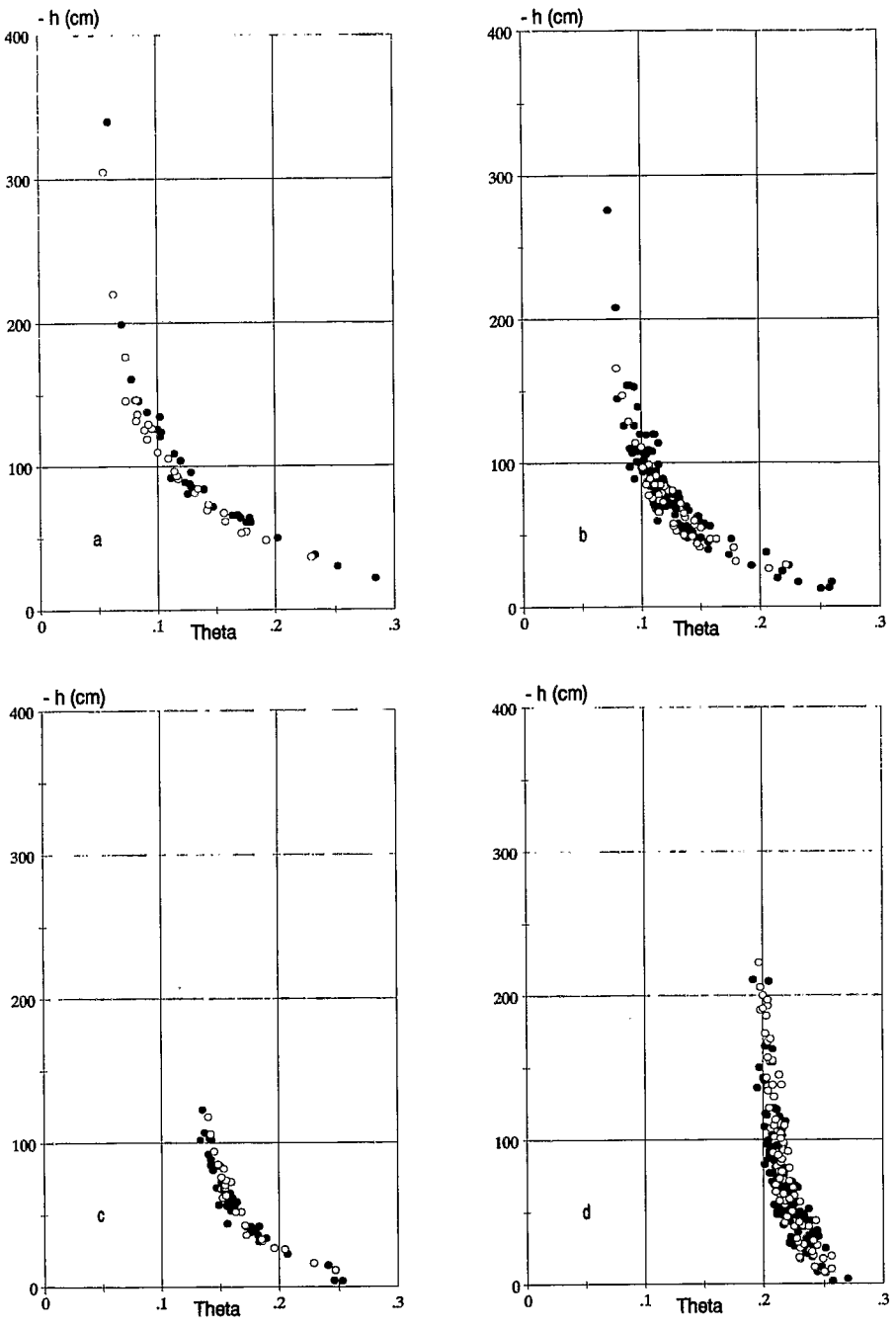

Fig. 2. $h(\theta)$ obtained from the simulated rain (open symbols) and ponded infiltration (solid symbols) experiments, for the different horizons distinguished in the profile.

TABLE 1

Paramters of eqn. (1) fitted to simulated rain data at $z = 10\,\text{cm}$ with $\theta_s = 0.26 + 0.01\,i$ ($i = 1, \ldots, 6$). θ_s and θ_r are in $\text{cm}^3\,\text{cm}^{-3}$, a is in cm^{-1}

θ_s	0.27	0.28	0.29	0.30	0.31	0.32
θ_r	0.0417	0.0407	0.0396	0.0387	0.0378	0.0369
a	−0.0206	−0.0218	−0.0231	−0.0244	−0.0258	−0.0272
b	2.570	2.504	2.447	2.398	2.354	2.316
c	0.611	0.601	0.591	0.583	0.575	0.568

of this parameter to be between 0.30 and 0.32. Considering the mean value $\theta_s = 0.31\,\text{cm}^3\,\text{cm}^{-3}$ to be a realistic estimate, fitting eqn. (1) on PI data gives $\theta_r = 0.040\,\text{cm}^3\,\text{cm}^{-3}$, $a = -0.024\,\text{cm}^{-1}$, $b = 2.368$ and $c = 0.578$. For the SR data, manual extrapolation for θ_s gives a value which lies between 0.27 and $0.32\,\text{cm}^3\,\text{cm}^{-3}$. Using six different values for $\theta_s = 0.26 + 0.01i$ ($i = 1, \ldots, 6$) and fitting eqn. (1) on SR data results in values summarised in Table 1 and shown on Fig. 3. Although the fitted parameters are sensitive to the value of θ_s, the resulting curves are hardly distinguishable in the range of observed data. In this type of experiment, the saturated water content might thus be estimated with up to 20% error. If this error in θ_s was acceptable for field purposes, it could influence greatly the determination of saturated hydraulic conductivity K_s. Soil conductivity varies greatly with water content, especially near saturation, 20% error on θ_s might result in several hundred percent error in K_s.

Equation (1) fitted to data for the three other horizons results in values shown in Table 2 and presented in Fig. 4. For each horizon, Table 2 gives also the maximum value of water content θ_{max} recorded during each experiment. Note that for $z \geqslant 60\,\text{cm}$, differences between θ_{max} values observed in each experiment are not significant, since the errors of measurement are of the same order. In Fig. 4 dotted curves are obtained from PI data, dashed ones from SR data and solid curves from both experiments. Table 2 and Fig. 4 confirm the preceding result: only the range of variation of the observed variables is affected by the water supply mode at the soil surface.

The K(θ) *relationship*

Points of this relation are obtained by applying Darcy's law with the underlying hypothesis of one dimensional vertical flow:

$$K = q/(1 - \partial h/\partial z)$$

where q and $\partial h/\partial z$ are flux density and water pressure gradient evaluated at

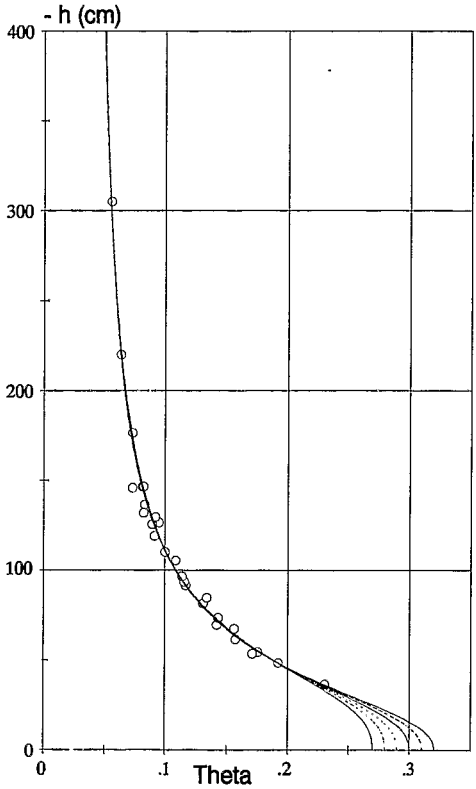

Fig. 3. Fitting eqn. (1) on data obtained from the simulated rain experiment at $z = 10$ cm with $\theta_s = 0.26 + 0.01i$ ($i = 1, \ldots, 6$).

time t_1 and depth z_1. Flux density is obtained by integrating the mass conservation law between depths z_1 and z_0:

$$q_{z0} - q_{z1} = \mathrm{d}W/\mathrm{d}t$$

where $W = \int_{z_0}^{z_1} \theta \mathrm{d}z$. During internal drainage conditions $q_{z_0} = z_0 = 0$, while under natural conditions choosing $z_0(t_1)$ such that $(\partial h/\partial z)_{z_0,t_1} = 1$ implies $q_{z0}(t_1) = 0$. In both cases, W represents the total water content of the profile between z_0 and z_1. Under internal drainage conditions $W(z_0, t)$ is correlated linearly with $\ln(t)$, and $q(z_1, t_1)$ is computed by simple differentiation. Note that in this case, only values of t corresponding to decreasing water contents at z_1 are considered. For all depths the coefficient of correlation r is greater than 0.95. The water pressure gradient is determined graphically from the water pressure profile $h(z, t_1)$.

Figures 5(a)–5(d) show, for the horizons already distinguished in the profile, points of $K(\theta)$ obtained from SR and PI experiments. As before, little

TABLE 2

Parameters of eqn. (1) fitted on simulated rain data (SR), double ring infiltrometer data (PI) and both experiments (SR + PI). θ_s, θ_r, and θ_{max} are in $cm^3\,cm^{-3}$, a is in cm^{-1}

z		SR	PI	SR + PI
10	θ_s	0.31	0.31	0.31
	θ_r	0.0378	0.0398	0.0385
	a	−0.0258	−0.0236	−0.0243
	b	2.354	2.368	2.374
	c	0.575	0.578	0.579
	θ_{max}	0.230	0.284	
20–40	θ_s	0.28	0.28	0.28
	θ_r	0.0489	0.0624	0.0606
	a	−0.0437	−0.0405	−0.0416
	b	1.993	2.141	2.121
	c	0.498	0.533	0.529
	θ_{max}	0.221	0.259	
60	θ_s	0.26	0.26	0.26
	θ_r	0.136	0.119	0.127
	a	−0.0493	−0.0482	−0.0487
	b	2.592	2.206	2.350
	c	0.614	0.547	0.574
	θ_{max}	0.246	0.253	
⩾80	θ_s	0.27	0.27	0.27
	θ_r	0.113	0.098	0.131
	a	−0.1409	−0.1063	−0.1164
	b	1.172	1.182	1.226
	c	0.147	0.154	0.184
	θ_{max}	0.265	0.269	

distinction could be made between points obtained from either experiment. However, the range of $K(\theta)$ values measured is sensitive to the method of water application. In particular for $z = 10\,cm$, while the maximum value determined from SR data does not exceed $0.8\,cm\,h^{-1}$, it is about $6\,cm\,h^{-1}$ when obtained from PI. Table 3 presents the equation which gave the best fit on the data obtained from both experiments for each horizon. These equations are also shown by the solid curves on Fig. 5. Note that for all horizons the saturated hydraulic conductivity is obtained by curve fitting. Note also that, for $z = 10\,cm$, points at lower water contents ($\theta < 0.08$) were not considered for the curve fitting. Were the saturated water content estimated to be $0.27\,cm^3\,cm^{-3}$ at $z = 10\,cm$, the resulting K_s would be about $2\,cm\,h^{-1}$, which is approximately an order of magnitude less than the actual value estimated for $\theta_s = 0.31\,cm^3\,cm^{-3}$.

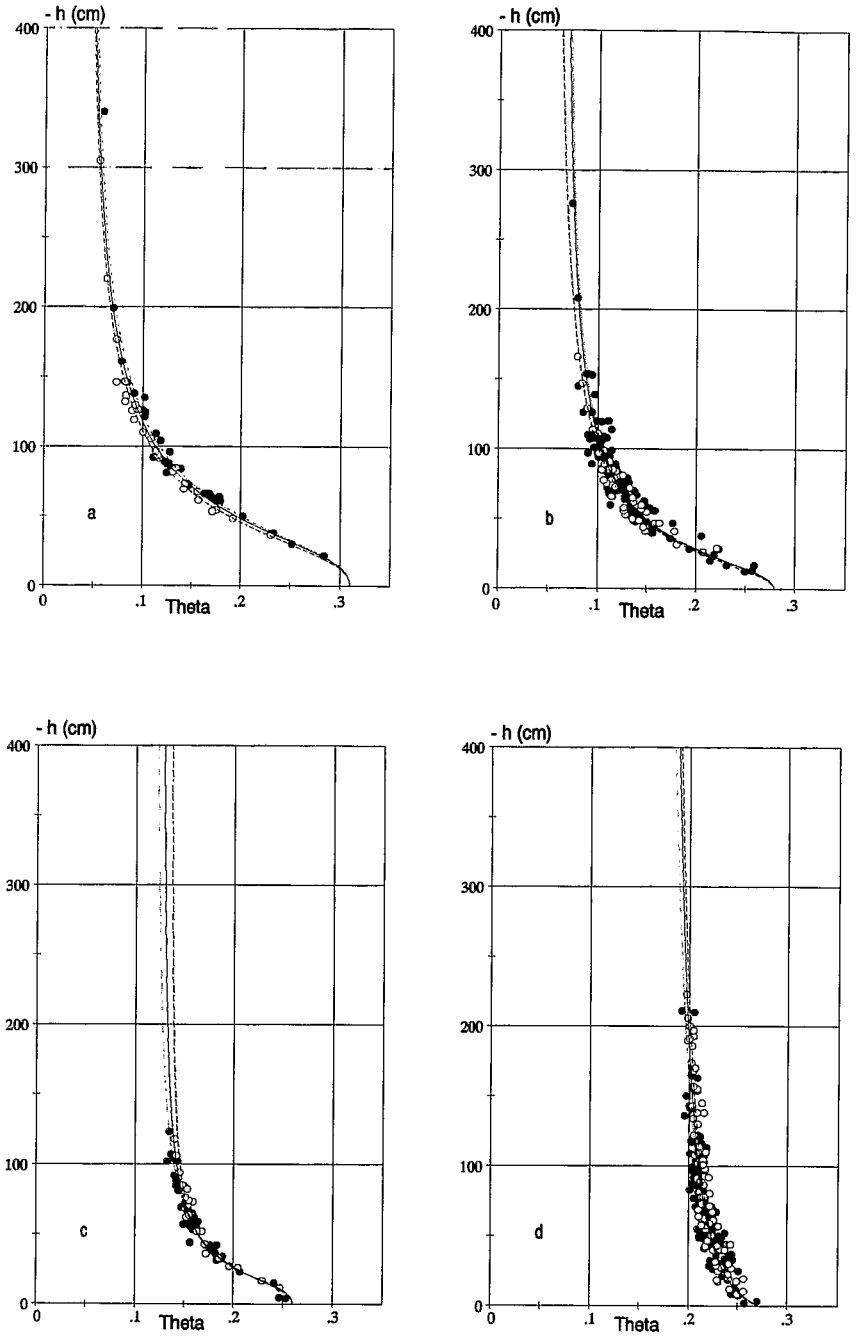

Fig. 4. Eqn. (1) fitted on data obtained from the simulated rain experiment (dashed lines), ponded infiltration (dotted lines) and both experiments (solid lines), for the various horizons in the profile.

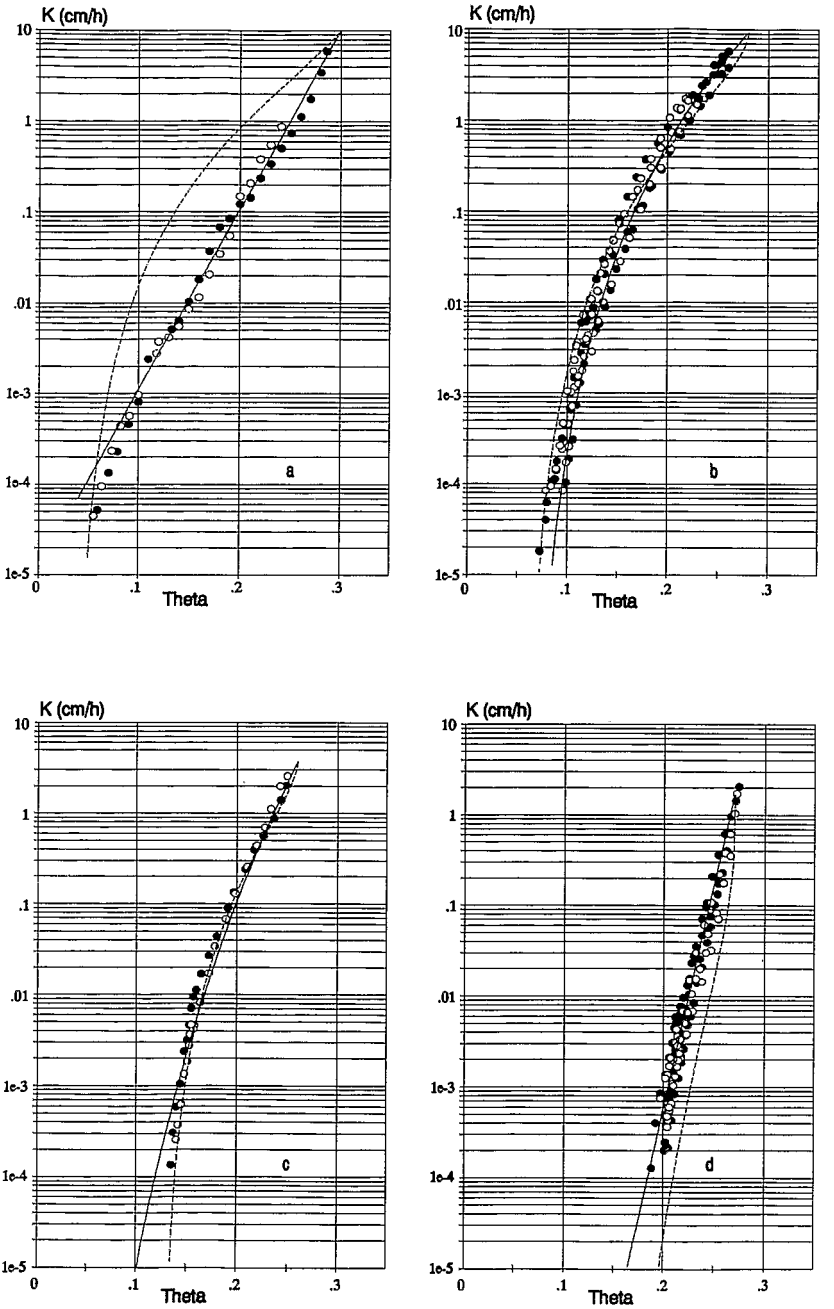

Fig. 5. $K(\theta)$ obtained from the simulated rain (open symbols) and ponded infiltration (solid symbols) experiments for the various horizons in the profile. Solid curves are the best fit on the data (see Table 3) Dashed curves are $K(\theta)$ predicted according to the model of Van Genuchten.

TABLE 3

Analytical expressions and the parameters that gave the best fit on $K(\theta)$ data obtained from both experiments for the various horizons in the profile. The saturated hydraulic conductivity K_s is determined by curve fitting. For each horizon, values of θ_s and θ_r are given in Table 2

z	Equation	K_s(cm h^{-1})	A
10	$K_s \cdot \exp(A(\theta - \theta_s)/(\theta_s - \theta_r))$	15.82	12.36
20–40	$K_s \cdot ((\theta - \theta_r)/(\theta_s - \theta_r))^A$	9.32	6.25
60	$K_s \cdot (\theta/\theta_s)^A$	3.69	13.58
$\geqslant 80$	$K_s \cdot \exp(A(\theta - \theta_s)/(\theta_s - \theta_r))$	1.68	15.85

Knowledge of the saturated hydraulic conductivity K_s and of parameters of $\theta(h)$ for each horizon, allows the prediction of $K(\theta)$ for each horizon, according to the model presented by Van Genuchten (1980). The predictions are shown by the dashed curves on Fig. 5. While the predicted relations are in fair accord with the observations in the intermediate horizons; they depart seriously from it in the uppermost and lowermost layers. This might be due to the sensitivity of predicted $K(\theta)$ to the value of θ_r as pointed out by Mualem (1976). Nevertheless, and whatever θ_s, θ_r and K_s are, the Van Genuchten model always gives an infinite slope $dK/d\theta$ at θ_s. This quantity, computed from eqn. (8) of Van Genuchten, with $\Theta = (\theta - \theta_r)/(\theta_s - \theta_r)$ contains a term of the form $(1 - \Theta^{1/c})^{c-1}$ and when θ reaches θ_s, this term becomes infinite unless b is negative which is impossible since in that case $\theta = \theta_r$ for $h = 0$. Note that not only the model of Van Genuchten yields an infinite slope $dK/d\theta$ at θ_s; the result will be the same for any model based on Mualem's theory (1976) where the analytical form of $h(\theta)$ is such that $\theta = \theta_s$ for, and only for, $h = 0$. This can be seen directly from eqn. (14) of Mualem. The physical basis of this fact is questionable, since θ_s is the 'natural saturation', (cf. Fig. 9 of Van Genuchten), generally less than the porosity (Vachaud et al., 1974). Were $dK/d\theta$ infinite at θ_s, it would be impossible to determine the hydraulic conductivity corresponding to the total saturation, which is not realistic since this parameter is actually measurable (Touma and Vauclin, 1986). As pointed out by one of the reviewers, the hydraulic conductivity at total saturation is not predicted by the model of Van Genuchten; this follows directly from the analytical expression of $h(\theta)$. Nevertheless, the question remains about the physical significance of the predicted $K(\theta)$. Stating the question differently: is the theory of Mualem realistic? If it is, is it physically sound to consider that $\theta = \theta_s$ for, and only for, $h = 0$; or must saturation be reached at some definite and negative value of h? The answer to this question is beyond the scope of this paper.

CONCLUSION

Comparison of data obtained from a rain simultor and a double ring infiltrometer shows that it is not possible to distinguish results inferred from either experiment. Nevertheless, the range of measurements corresponding to the double ring infiltrometer is wider than that resulting from the rain simulator, especially for higher water contents. In the upper soil horizons, the saturated water content may be underestimated by up to 20% using the rain simulator, while underestimation of the saturated hydraulic conductivity may reach an order of magnitude. Most probably, this is due to crusting of the soil surface under simulated rain. Thus, it appears that, for such soils, the double ring infiltrometer is more suitable than the rain simulator to determine the soil hydrological properties, even though this latter device is essential to study infiltration capacity and runoff.

The measured hydraulic conductivity–water content relationships were compared with those predicted according to the model of Van Genuchten (1980). Comparison showed fair accord for some soil horizons but not for others. Further, the predicted curves always show an infinite slope for the saturated water content, which is not physically realistic.

REFERENCES

Agassi, M., Shainberg, I. and Morin, J., 1981. Effect of electrolyte concentration and soil sodicity on the infiltration rate and crust formation. Soil Sci. Soc. Am. J., 45: 848–851.

Agassi, M., Morin, J. and Shainberg, I., 1982. Laboratory studies of infiltration and runoff control in semi-arid soils in Israel. Geoderma, 28: 345–356.

Ahuja, L.R., El-Swaify, S.A. and Rahman, A., 1976. Measuring hydrologic properties of soil with a double-ring infiltrometer and multiple-depth tensiometers. Soil Sci. Soc. Am. J., 40: 494–499.

Arya, L.M., Farrell, D.A. and Blake, G.R., 1975. A field study of the soil water depletion patterns in presence of growing soybean roots. I. Determination of hydraulic properties of the soil. Soil Sci. Soc. Am. Proc., 39: 424–430.

Asseline, J. and Valentin, C., 1978. Construction et mise au point d'un infiltromètre à aspesion. Cah. ORSTOM, Ser. Hydrol., 15: 321–345.

Bach, L.B., Wierenga, P.J. and Ward, T.J., 1986. Estimation of the Philip infiltration parameters from rainfall simulation data. Soil Sci. Soc. Am. J., 50: 1319–1323.

Ben-Hur, M., Shainberg, I. and Morin, J., 1987. Variability of infiltration in a field with surface-sealed soil. Soil Sci. Soc. Am. J., 51: 1299–1302.

Bernard, A., 1987. Le simulateur de pluie 2ème génération. Note technique. ORSTOM, Montepellier.

Bridge, B.J. and Ross, P.J., 1985. A portable microcomputer-controlled drip infiltrometer. II. Field measurement of sorptivity, hydraulic conductivity and time to ponding. Aust. J. Soil Res., 23: 393–404.

Bryan, R.B. and De Ploey, J., 1983. Comparability of soil erosion measurements with different laboatory rainfall simulators. In: J. De Ploey (Editor), Rainfall simulation, runoff and soil erosion. CATENA Supplement 4, Braunschweig.

Casenave, A., 1982. Le minisimulateur de pluie. Conditions d'utilisation et principes d'interprétation des résultats. Cah. ORSTOM, Ser. Hydrol., 29: 207–227.

Chong, S.K., Green, R.E., and Ahuja, L.R., 1981. Simple in situ determination of hydraulic conductivity by power function descriptions of drainage. Water Resour. Res., 17: 1109–1114.

Gardner, W.R., 1958. Some steady state solutions of the unsaturated moisture flow equation with application to evaporation from a water table. Soil Sci., 85: 228–232.

Hardy, N., Shainberg, I., Gal, M. and Keren, R., 1983. The effect of water quality and storm sequence upon infiltration rate and crust formation. J. Soil. Sci., 34: 665–676.

Hillel, D., Krentos, V.D. and Stilianou, Y., 1972. Procedure and test of an internal drainage method for measuring soil hydraulic characteristics in situ. Soil Sci., 114: 395–400.

Jeppson, R.W., Rawls, W.J., Hamon, W.R. and Schreiber, D.L., 1975. Use of axisymmetric infiltration model and field data to determine hydraulic properties of soils. Water Resour. Res., 11: 127–137.

Julander, R.P. and Jackson, W., 1983. Drop former and double ring infiltrometers. A comparison. Proceedings of the National Conference on Advances in Infiltration; ASAE, New York, pp. 249–253.

Levy, G., Shainberg, I. and Morin, J., 1986. Factors affecting the stability of soil crusts in subsequent storms. Soil Sci. Soc. Am J., 50: 196–201.

Marquardt, D.W., 1963. An algorithm for least squares estimation of nonlinear parameters. J. Soc. Indust. Appl. Math., 11: 431–441.

Miller, W.P., 1987. Infiltration and soil loss of three gypsum-amended ultisols under simulated rainfall. Soil Sci. Soc. Am. J., 51: 1314–1320.

Mualem, Y., 1976. A new model for predicting the hydraulic conductivity of unsaturated porous media. Water Resour. Res., 12: 513–522.

Remley, P.A. and Bradford, J.M., 1989. Relationship of soil crust morphology to inter-rill erosion parameters. Soil Sci. Soc. Am. J., 53: 1215–1221.

Sharma, P.P., Gantzer, C.J. and Blake, G.R., 1981. Hydraulic gradients across simulated rain-formed soil surface seals. Soil Sci. Soc. Am. J., 45: 1031–1034.

Swartzendruber, D. and Hillel, D., 1975. Infiltration and runoff for small field plots under constant intensity rainfall. Water Resour. Res., 11: 445–451.

Touma, J., 1984. Etude critique de la caractérisation hydrodynamique des sols non saturés: rôle de l'air, influence de l'écoulement multidimensionnel de l'eau. Thèse de Docteur ès Sciences Physiques, Université de Grenoble, 190 pp.

Touma, J. and Vauclin, M., 1986. Experimental and numerical analysis of two-phase infiltration in a partially saturated soil. Transp. porous media, 1: 27–55.

Vachaud, G., Gaudet, J.P. and Kuraz, V., 1974. Air and water flow during ponded infiltration in a vertical bounded column of soil. J. Hydrol., 22: 89–108.

Vachaud, G., Dancette, C., Sonko, M. and Thony, J.L., 1978. Méthodes de caractérisation des caractéristiques hydrodynamiques d'un sol non saturé in-situ. Ann. Agron., 29: 1–36.

Van Genuchten, M. Th., 1980. A closed-form equation for predicting the hydraulic conductivity of unsaturated soils. Soil Sci. Soc. Am. J., 44: 892–898.

Vauclin, M., Imbernon, J., Vachaud, G. and Dancette, C., 1983. Description expérimentale et modélisation stochastique des transferts par la mise en échelle des propriétés hydrodynamiques des sols. Isotope and radiation techniques in soil physics and irrigation studies. IAEA-SM-267/25, pp. 103–124.

Vieira, S.R., Nielsen, D.R. and Biggar, J.W., 1981. Spatial variability of field-measured infiltration rate. Soil Sci. Soc. Am. J., 45: 1040–1048.

Youngs, E.G., 1986. Estimating hydraulic conductivity values from ring infiltrometer measurements. J. Soil Sci., 38: 623–632.